9-4-2019

Force Oscillations Distort Avalanche Shapes

Louis W. McFaul
University of Illinois at Urbana-Champaign

Wendelin J. Wright
wendelin@bucknell.edu

Jordan Sickle
University of Illinois at Urbana-Champaign

Karin A. Dahmen
University of Illinois at Urbana-Champaign

Materials Research Letters

ISSN: (Print) 2166-3831 (Online) Journal homepage: https://www.tandfonline.com/loi/tmrl20

Force oscillations distort avalanche shapes

Louis W. McFaul, Wendelin J. Wright, Jordan Sickle & Karin A. Dahmen

To cite this article: Louis W. McFaul, Wendelin J. Wright, Jordan Sickle & Karin A. Dahmen (2019) Force oscillations distort avalanche shapes, Materials Research Letters, 7:12, 496-502, DOI: 10.1080/21663831.2019.1659437

To link to this article: https://doi.org/10.1080/21663831.2019.1659437

Published online: 04 Sep 2019.

MATER. RES. LETT.
2019, VOL. 7, NO. 12, 496–502
https://doi.org/10.1080/21663831.2019.1659437

MATERIALS RESEARCH LETTERS
Taylor & Francis
Taylor & Francis Group

REPORT

Force oscillations distort avalanche shapes

Louis W. McFaul [a], Wendelin J. Wright [b,c], Jordan Sickle[a] and Karin A. Dahmen[a]

[a]Physics and Institute of Condensed Matter Theory, University of Illinois at Urbana Champaign, Urbana, IL, USA; [b]Mechanical Engineering, Bucknell University, Lewisburg, PA, USA; [c]Chemical Engineering, Bucknell University, Lewisburg, PA, USA

ABSTRACT

Contradictory scaling behavior in experiments testing the principle of universality may be due to external oscillations. Thus, the effect of damped oscillatory external forces on slip avalanches in slowly deformed solids is simulated using a mean-field model. Akin to a resonance effect, oscillatory driving forces change the dynamics of avalanches with durations close to the oscillation period. This problem can be avoided by tuning mechanical resonance frequencies away from the range of the inverse avalanche durations. The results provide critical guidance for experimental tests for universality and a quantitative understanding of avalanche dynamics under a wide range of driving conditions.

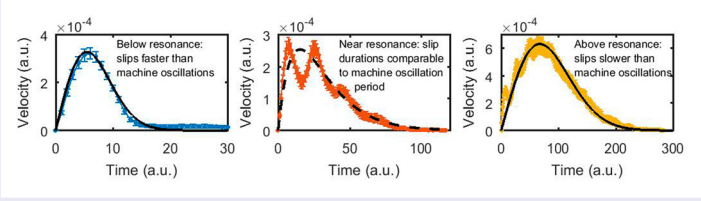

IMPACT STATEMENT

Simulations of deformation show how commonly neglected errant oscillations distort the dynamics of discrete plastic events and how the effects of these oscillations can be mitigated in experiments and applications.

ARTICLE HISTORY
Received 22 July 2019

KEYWORDS
Plasticity; avalanches; criticality; scaling behavior; oscillations

Introduction

At low strain- or stress rates, many solids deform intermittently with sudden 'slip-avalanches', similar to earthquakes. Theory and experiments probe *universality*, i.e. whether different materials show the same scaling behavior for avalanche statistics and dynamics, irrespective of the microscopic details [1–10], and in a variety of systems [11–16]. Universality, if it exists, is a powerful tool for the prediction of materials properties and establishing guidelines for experimental design. Thus far, studies have focused almost exclusively on fixed strain-rate or stress-rate deformation, sometimes reporting contradictory scaling behaviors. All of these studies, however, have neglected the effects of oscillations in the imposed load or displacement signal, which is a critical omission for two reasons: (1) real systems inherently experience oscillations, and (2) as we show herein, ignoring oscillations in the data can skew the experimental results, potentially leading to the false conclusion that related systems have different scaling behavior. Simply put, ignoring oscillations may obscure the observation of universality across materials systems.

Prior studies of slip avalanches have usually ignored oscillations despite their common occurrence in real systems [17–19]; here we employ a mean-field model of slipping weak spots [1,6] to understand the effect of oscillations on slip avalanches. We choose this model because (1) it is confirmed by many recent experiments [8], (2) it is currently the *only model available* that predicts more than 12 different statistical properties observed in experiments on bulk metallic glasses [8,20,21] in the absence of oscillations, (3) experimental results on a wide range of scales (nanocrystals, granular materials, and earthquakes [5,22–24]) also agree with the model predictions, (4) renormalization group treatments imply that the model is even more widely applicable [1,6], and (5) the model

CONTACT Karin A. Dahmen dahmen@illinois.edu Physics and Institute of Condensed Matter Theory, University of Illinois at Urbana Champaign, 1110 West Green Street, Urbana, IL 61801, USA

is analytically solvable, and its simplicity affords crucial intuition for predictions, design, and new approaches to data analysis.

By imposing an oscillation on an otherwise monotonic driving force, we show that the model predicts that these oscillations can distort average temporal profiles of the avalanche propagation velocities. These distortions are most apparent at 'resonance', i.e. when the duration of the avalanches is comparable to the period of the oscillations. Thus recognition and proper treatment of oscillations in experimental load and displacement signals is essential.

The drive toward device miniaturization requires quantitative information on slip avalanche behavior at the nanoscale (e.g. [15,25]). At these length scales, the effects of oscillations may be magnified and distort the true materials behavior. Oscillations may arise when a sudden slip event occurs, initiating an event that reverberates throughout the contact. Indeed the nanoindenter was not developed with the intention of measuring the dynamics of rapid plasticity events, so the available instrumentation is evolving to meet these challenges. In this work, we develop the requisite theory to predict and explain avalanche dynamics in the presence of oscillations. A follow-up paper will analyze experimental avalanche shapes under this theoretical framework [26,27].

Avalanche shapes in the mean-field model

The mean-field avalanche model predicts the scaling behavior of the distributions of avalanche sizes, durations, propagation velocities, and dynamics [6,28,29]. These scaling predictions have been tested in experimental avalanche data [8,23,30]. The model also predicts the average 'avalanche shape', either for avalanches of a similar duration or a similar size. The term 'avalanche shape' refers to the average temporal profile of the avalanche velocity. While the propagation velocity of individual avalanches fluctuates greatly, these *average* avalanche shapes are predicted to be specific smooth scaling functions of velocity versus time. The average avalanche shape for avalanches of a similar duration (the 'duration-binned avalanche shape') is predicted to be an inverted parabola [31–33], but the average avalanche shape for avalanches of a similar size (the 'size-binned avalanche shape') is predicted to follow a function $f\ (t) = \mathrm{A}^{*}\mathrm{t}^{*}\exp(-\mathrm{B}^{*}t^2)$ for non-universal constants A and B [28,31] with time t. This specific size-binned scaling function has also been tested in experimental data, with excellent agreement in some cases [8,30,34] but with deviations in others that in hindsight may be explained by inadvertently introduced forced oscillations [25]. Given that the model's scaling functions are powerful predictions for experiments (more stringent than single-valued experimentally-fitted power law exponents), we must understand how these scaling functions may change with physically realistic external forcing other than a linear force increase.

We find that oscillations in the applied force affect the average avalanche shapes. The model discretizes the shear band into small cells. In previous studies, the avalanches were triggered by monotonically increasing applied stress (or strain). When the least-stable cell yields, it can trigger other cells to yield in a chain-reaction-like avalanche until all cells are stable and the avalanche ends. For the slow driving case, the average applied stress does not increase while an avalanche is ongoing. To study the effect of oscillations, however, rather than linearly increasing the applied stress with time, we instead take the imposed boundary displacement (and thus the resulting stress) to be an exponentially-damped sinusoid that starts concurrently with the beginning of the avalanche and continues while the avalanche is ongoing. The oscillation amplitude decays to zero after several oscillation periods.

In the mean-field model, the local stress on each cell has two contributions: the stress from the neighboring cells and the externally-imposed stress. The stress from the neighboring cells on the i^{th} cell is $\frac{J}{N}\sum_j(u_j - u_i)$, where J/N is the mean-field elastic coupling between cells and u_j is the position of the j^{th} cell. The external stress on the i^{th} cell is $K_L(u_0 - u_i)$, where K_L is the stiffness of the boundary spring and u_0 is the equilibrium position of the cells due to the force of the boundary spring. This local stress τ_i on the i^{th} cell therefore obeys the equation:

$$\tau_i = \frac{J}{N}\sum_j(u_j - u_i) + K_L(u_0 - u_i)$$

The model dynamics depend on J and K_L through the stress conservation parameter $c = \frac{J}{J+K_L}$; see [6,29,35] for details. We simulate $N = 5 \times 10^5$ cells for $c = 1 - \frac{1}{\sqrt{N}}$ [35,36]. For slow monotonic driving, the equilibrium position u_0 increases linearly with time t as $u_0 = vt$, where the rate v is slow compared to the rate at which avalanches propagate. To include applied-force oscillations we take u_0 to be an exponentially damped sinusoid: $u_0 = Ae^{-t/\theta}\sin(\omega t)$ with amplitude A, frequency ω, and decay time θ. The damped oscillation amplitude $A = 10/N$ in units of simulation stress divided by loading stiffness K_L, period $2\pi/\omega = 100$, and decay constant $\theta = 114$, both in units of simulation timesteps.

Figure 1 shows that in the presence of oscillations the simulated average avalanche shapes look somewhat similar to the shapes obtained for monotonic driving but with additional oscillations. To compute these average

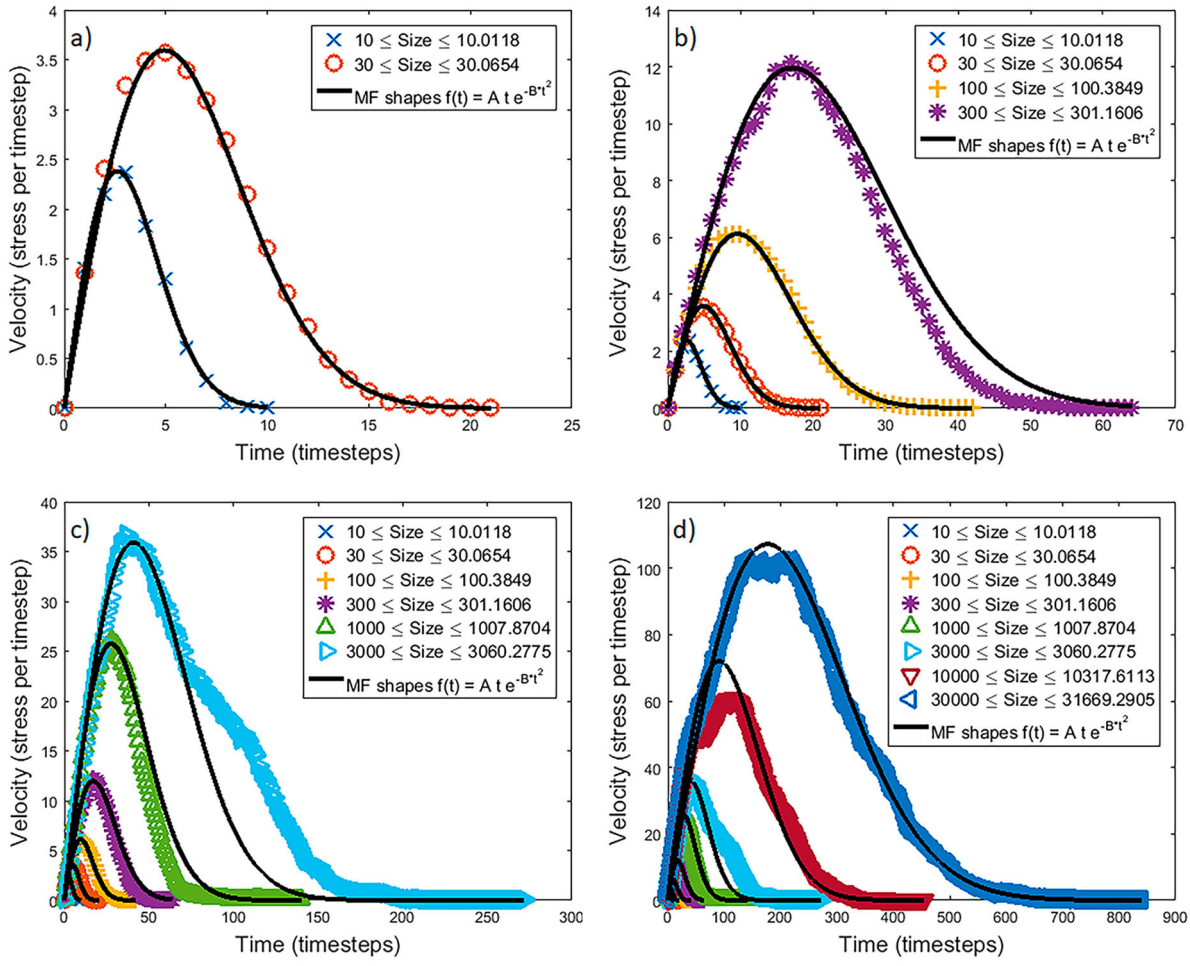

Figure 1. Simulated avalanche shapes (averaged over 250 avalanches of given avalanche size), for oscillating sample boundary (oscillation period 100 time steps). (a) Shapes for avalanche durations of roughly 1/10 of the oscillation period. The shapes agree with the mean-field shape for monotonic driving (black line). (b) The avalanches in the two additional shapes have durations of about ½ the oscillation period. The corresponding shapes deviate from the shape for monotonic driving. (c) Two additional shapes correspond to durations of about 1–2 oscillation periods; they again deviate from the monotonically driven case. (d) Durations of the additional shapes are on the order of multiple oscillation periods; their shapes agree with those of the monotonic case.

avalanche shapes for avalanches of a certain size, the velocity versus time profiles of avalanches of a similar size are averaged. (The size is proportional to the sum of the total distances that the simulated cells move during a particular avalanche.)

The oscillation-affected shapes differ in important ways from those obtained for monotonic driving. Figure 1 shows simulated average avalanche shapes for different avalanche sizes. In each subfigure, the black curve follows the predicted shape function $u_0(t) = Ate^{-Bt^2}$ for monotonic driving where A and B are non-universal constants [6,28]. In the following we show that avalanches with durations T that are either short or long compared to the oscillation period $2\pi/\omega$ follow the mean-field shape for monotonic driving, while avalanches with durations that are similar to the oscillation period are distorted by the oscillations, similar to a resonance effect. We compare the shapes to these reference functions to clarify our observations:

(a) $T \ll 2\pi/\omega$:

Figure 1(a) shows the average avalanche shapes computed for the two *smallest-size* bins; these shapes closely follow the mean-field prediction obtained for monotonic driving. This result is expected because the durations of most of the avalanches in these bins are about an order of magnitude shorter than the period of oscillation (100 timesteps).

(b) $T \sim 2\pi/\omega$:

Figure 1(b) shows the average avalanche shapes for two larger size bins that contain avalanches mainly with

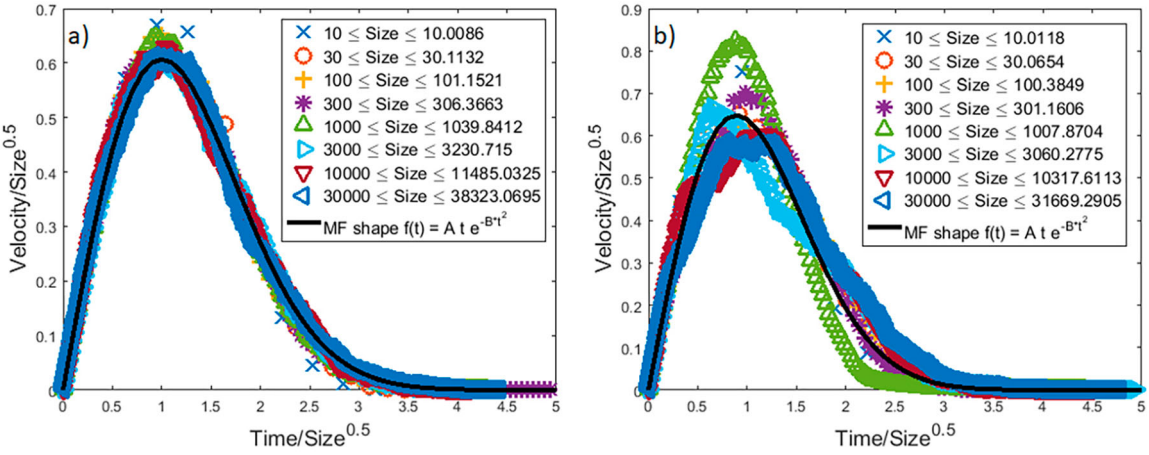

Figure 2. Attempted shape collapses for size-binned avalanche shapes, averaged over 250 avalanches each. (a) High-quality collapse onto the predicted scaling function for constant boundary velocity. (b) Low-quality collapse for oscillatory boundary motion (see Figure 1 for uncollapsed shapes).

durations on the order of half of the oscillation period. These shapes begin to deviate from the monotonic-driving shape prediction, with a steeper slope than predicted.

(c) $T \sim 2\pi/\omega$:

Figure 1(c) shows average avalanche shapes for two even larger size bins that contain avalanches with durations on the order of 1–2 oscillation periods. These average shapes again deviate from the monotonic-driving shape, with downward slopes that are either abnormally steep or abnormally shallow. A signature of the oscillation period is observable as the 'ledge' or 'shoulder' in the average shape of the size-3000-avalanches near a time of 100 timesteps.

(d) $T \gg 2\pi/\omega$:

Figure 1(d) shows average avalanche shapes for the two largest size bins, whose avalanches propagate for several oscillation periods. Apart from some slight rounding at the top of the largest-size average shape, this shape again follows the shape for monotonic-driving, as in (a).

We observe that when the oscillation period and the avalanche durations are similar in length then the oscillations distort the mean-field size-binned shape so that it deviates from the shape obtained for monotonic driving. The mid-size average avalanche shapes (which contain avalanches with durations roughly on the order of half an oscillation period to a few oscillation periods) have tails that are distorted compared to the mean-field shape function for monotonic driving. The reason is that in this case the oscillations dynamically interact with the ongoing avalanche.

This finding is also supported by the corresponding scaling collapses in Figure 2(a and b). Figure 2(a) shows the shape collapse for monotonic driving; the shapes collapse onto each other and onto the mean-field shape function. In contrast, Figure 2(b) shows that for oscillatory stresses the shapes no longer collapse.

Figure 3 shows that the corresponding scatterplots of avalanche duration T versus size S without oscillations (Figure 3(a)) and with oscillations (Figure 3(b)) both agree well with the predicted $T \sim S^{1/2}$ scaling law. Figure 3(c) shows the complementary cumulative distribution function (CCDF) for the avalanche sizes S. Without oscillations, it follows the expected –0.5 power law. In contrast, with oscillations it deviates from a power law, but in a hypothetical or experimental dataset with instrumental noise superimposed on the avalanche signal, such a CCDF may be misinterpreted as following a power law with a wrong exponent (of roughly 0.6 instead of 0.5 for these simulation parameters). Figure 3(d) shows a similar distortion for the duration CCDF, which (with noisier data) could also be misinterpreted as a power law with a modified exponent (roughly 1.1 instead of 1.0 for these simulation parameters).

Implications for experiments

The model predicts that oscillations *may not be relevant to the avalanche-propagation dynamics, if the avalanche durations are either short or long compared to the oscillation period*. In experiments, the effect of the oscillations will therefore depend on how well these timescales match. For example, in some micropillar compression experiments, there may be a large mismatch between the avalanche durations and the period of oscillations so that the oscillations have little effect

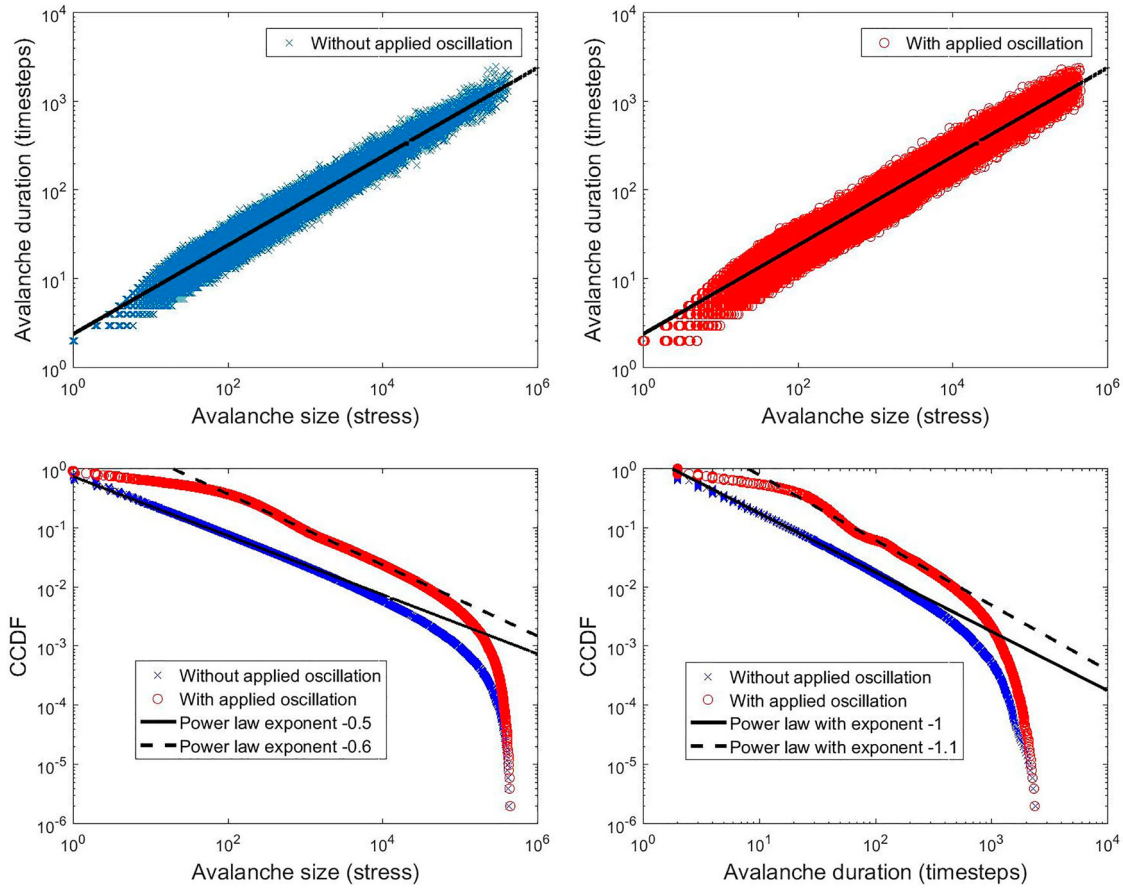

Figure 3. Size and duration scaling of avalanches. (a) Duration T vs. size S scatterplot for monotonically-increasing stress, agrees with prediction $T \sim S^{1/2}$ (black line). (b) T vs. S for an oscillating boundary, agrees with prediction $T \sim S^{1/2}$. (c) CCDF of avalanche sizes without (blue x) and with (red o) an oscillating boundary. (d) CCDF of avalanche durations without (blue x) and with (red o) an oscillating boundary. In (c) and (d), the oscillatory-model CCDFs may be mistaken for power laws with the wrong exponents (dashed line).

on avalanche-propagation dynamics [26,27]. In other experiments, however, oscillations distort the avalanche dynamics so much, that by neglecting their effect, non-universality can falsely be inferred [15,25–27].

The key message of this paper, i.e. that stress- or strain-oscillations distort those avalanches with durations on the order of the oscillation period, is widely applicable. Details on the specifics of the shape distortion in any real experiment depend on the specific form of the resonant oscillation (e.g. its amplitude and decay constants, frequencies, and excitation mode). The numerical values of the apparent power-law deviations in Figure 3(c and d) are also not universal predictions; rather the power-law deviations will depend on the specific resonance characteristics of an actual experimental system. Our point then is to show that if similar deviations are observed in experiments, oscillations may be the underlying cause, rather than deviation from universality.

The lesson for experimental design is simple: compare the timescales of the avalanches to the timescales of the boundary oscillation, and if they are on the same order of magnitude, then the experiment should be modified in order to separate the timescales. This can be accomplished either by tuning the oscillation period of the experimental setup (e.g. machine stiffness, sample size, etc., if possible), or by choosing a specimen that yields avalanche durations compatible with (i.e. an order of magnitude either larger or smaller than) the applied-force oscillation period. The range of avalanche durations in a compression experiment may be adjustable by changing the cross-sectional area and height of the specimens.

Conclusions

Resonant oscillations affect avalanche dynamics, especially for avalanches with durations comparable to the period of the mechanical resonance of the experimental setup. For avalanche durations that are long (or short) compared to the resonant period, the simulated average avalanche shape reverts to the mean-field shape prediction for monotonic driving. For experiments the results imply that a comparison of the resonant oscillation period of the experimental system to

the avalanche durations is necessary for correct interpretation of the data. To obtain undistorted avalanche shapes, it is important to tune the oscillation period away from the avalanche durations. The results further imply that avalanche shapes can be used to identify subtle oscillations in the driving force and their frequency. Our findings are relevant also to other avalanching systems, including magnets [27,32,34,37,38] and earthquakes [39,40].

Acknowledgments

We thank Robert Maaß and Gregory Sparks for helpful conversations and experimental data [27]. This work was supported by NSF CBET 1336634, the Heinemann Family Professorship at Bucknell University, and NSF PHY17-48958.

Disclosure statement

No potential conflict of interest was reported by the authors.

Funding

This work was supported by National Science Foundation: [Grant Number NSF CBET 1336634,NSF PHY17-48958] and the Heinemann Family Professorship at Bucknell University.

ORCID

Louis W. McFaul http://orcid.org/0000-0003-1554-2729
Wendelin J. Wright http://orcid.org/0000-0001-6493-6025

References

[1] Fisher DS, Dahmen K, Ramanathan S, et al. Statistics of earthquakes in simple models of heterogeneous faults. Phys Rev Lett. 1997;78(25):4885–4888.
[2] Miguel M-C, Vespignani A, Zapperi S, et al. Intermittent dislocation flow in viscoplastic deformation. Nature. 2001;410:667–671.
[3] Koslowski M, LeSar R, Thomson R. Avalanches and scaling in plastic deformation. Phys Rev Lett. 2004;93(12):125502.
[4] Dimiduk DM, Woodward C, LeSar R, et al. Scale-free intermittent flow in crystal plasticity. Science. 2006;312:1188–1190.
[5] Zaiser M. Scale invariance in plastic flow of crystalline solids. Adv Phys. 2006;55(1–2):185–245.
[6] Dahmen KA, Ben-Zion Y, Uhl JT. Micromechanical model for deformation in solids with universal predictions for stress-strain curves and slip avalanches. Phys Rev Lett. 2009;102(17):175501.
[7] Maaß R, Derlet PM, Greer JR. Small-scale plasticity: insights into dislocation avalanche velocities. Scr Mater. 2013;69(8):586–589.
[8] Antonaglia J, Wright WJ, Gu XJ, et al. Bulk metallic glasses deform via slip avalanches. Phys Rev Lett. 2014;112(15):155501.
[9] Ispánovity PD, Laurson L, Zaiser M, et al. Avalanches in 2D dislocation systems: plastic yielding is not depinning. Phys Rev Lett. 2014;112(23):235501.
[10] Papanikolaou S, Cui Y, Ghoniem N. Avalanches and plastic flow in crystal plasticity: an overview. Model Simul Mater Sci Eng. 2017;26:013001.
[11] Pan Y, Wu H, Wang X, et al. Rotatable precipitates change the scale-free to scale dependent statistics in compressed Ti nano-pillars. Sci Rep. 2019;9:3778.
[12] Pelusi F, Sbragaglia M, Benzi R. Avalanche statistics during coarsening dynamics. Soft Matter. 2019;15:4518–4524.
[13] Romero FJ, Martín-Olalla J-M, Gallardo MC, et al. Scale-invariant avalanche dynamics in the temperature-driven martensitic transition of a Cu-Al-Be single crystal. Phys Rev B. 2019;99(22):224101.
[14] Song H, Dimiduk D, Papanikolaou S. Universality class of nanocrystal plasticity: localization and self-organization in discrete dislocation dynamics. Phys Rev Lett. 2019;122(17):178001.
[15] Sparks G, Maaß R. Effects of orientation and pre-deformation on velocity profiles of dislocation avalanches in gold microcrystals. Eur Phys J B. 2019;92:15.
[16] Zreihan N, Faran E, Vives E, et al. Relations between stress drops and acoustic emission measured during mechanical loading. Phys Rev Mater. 2019;3(4):043603.
[17] Gomberg J, Reasenberg PA, Bodin P, et al. Earthquake triggering by seismic waves following the Landers and Hector Mine earthquakes. Nature. 2001;411:462–466.
[18] Johnson PA, Jia X. Nonlinear dynamics, granular media and dynamic earthquake triggering. Nature. 2005;437:871–874.
[19] Arioli G, Gazzola F. A new mathematical explanation of what triggered the catastrophic torsional mode of the Tacoma Narrows Bridge. App Math Model. 2015;39(2):901–912.
[20] Antonaglia J, Xie X, Schwarz G, et al. Tuned critical avalanche scaling in bulk metallic glasses. Sci Rep. 2014;4:4382.
[21] Wright WJ, Liu Y, Gu XJ, et al. Experimental evidence for both progressive and simultaneous shear during quasistatic compression of a bulk metallic glass. J App Phys. 2016;119:084908.
[22] Friedman N, Jennings AT, Tsekenis G, et al. Statistics of dislocation slip avalanches in nanosized single crystals show tuned critical behavior predicted by a simple mean field model. Phys Rev Lett. 2012;109(9):095507.
[23] Uhl JT, Pathak S, Schorlemmer D, et al. Universal quake statistics: from compressed nanocrystals to earthquakes. Sci Rep. 2015;5:16493.
[24] Sethna JP, Bierbaum MK, Dahmen KA, et al. Deformation of crystals: connections with statistical physics. Ann Rev Mater Res. 2017;47:217–246.
[25] Sparks G, Maaß R. Shapes and velocity relaxation of dislocation avalanches in Au and Nb microcrystals. Acta Mater. 2018;152:86–95.
[26] McFaul LW, Sparks G, Sickle J, et al. Submitted.
[27] McFaul LW. Temporal properties of avalanche dynamics [Ph.D. thesis]. University of Illinois at Urbana-Champaign; 2019.

[28] Fisher DS. Collective transport in random media: from superconductors to earthquakes. Phys Rep. 1998;301: 113–150.
[29] LeBlanc M. Avalanches in plastic deformation: maximum velocity statistics, finite temperature effects, and analysis of low time resolution data [Ph.D. thesis]. University of Illinois at Urbana-Champaign; 2016.
[30] Sheikh MA, Weaver RL, Dahmen KA. Avalanche statistics identify intrinsic stellar processes near criticality in KIC 8462852. Phys Rev Lett. 2016;117(26):261101.
[31] Sethna JP, Dahmen KA, Myers CR. Crackling noise. Nature. 2001;410:242–250.
[32] Papanikolaou S, Bohn F, Sommer RL, et al. Universality beyond power laws and the average avalanche shape. Nat Phys. 2011;7:316–320.
[33] Baldassarri A, Colaiori F, Castellano C. Average shape of a fluctuation: universality in excursions of stochastic processes. Phys Rev Lett. 2003;90(6):060601.
[34] Durin G, Bohn F, Corrêa MA, et al. Quantitative scaling of magnetic avalanches. Phys Rev Lett. 2016;117(8):087201.
[35] Dahmen KA, Ertas D, Ben-Zion Y. Gutenberg-Richter and characteristic earthquake behavior in simple mean-field models of heterogeneous faults. Phys Rev E. 1998;58(2):1494–1501.
[36] Dahmen KA, Ben-Zion Y, Uhl JT. A simple analytic theory for the statistics of avalanches in sheared granular materials. Nat Phys. 2011;7:554–557.
[37] Sethna JP, Dahmen K, Kartha S, et al. Hysteresis and hierarchies: dynamics of disorder-driven first-order phase transformations. Phys Rev Lett. 1993;70(21): 3347–3350.
[38] O'Brien KP, Weissman MB. Statistical characterization of Barkhausen noise. Phys Rev E. 1994;50(5):3446–3452.
[39] Wilcock WSD. Tidal triggering of earthquakes in the Northeast Pacific Ocean. Geophys J Int. 2009;179(2): 1055–1070.
[40] Brinkman BAW, LeBlanc M, Ben-Zion Y, et al. Probing failure susceptibilities of earthquake faults using small-quake tidal correlations. Nat Commun. 2015;6: 6157.